

# Storage-Ring Measurement of the Hyperfine Induced $^{47}\text{Ti}^{18+} (2s2p^3P_0 \rightarrow 2s^2^1S_0)$ Transition Rate

S. Schippers, E. W. Schmidt, D. Bernhardt, D. Yu,\* and A. Müller

*Institut für Atom- und Molekülphysik, Justus-Liebig-Universität, 35392 Giessen, Germany*

M. Lestinsky, D. A. Orlov, M. Grieser, R. Repnow, and A. Wolf

*Max-Planck-Institut für Kernphysik, 69117 Heidelberg, Germany*

(Received 12 October 2006; published 18 January 2007)

The hyperfine induced  $2s2p^3P_0 \rightarrow 2s^2^1S_0$  transition rate  $A_{\text{HFI}}$  in berylliumlike  $^{47}\text{Ti}^{18+}$  is measured. Resonant electron-ion recombination in a heavy-ion storage ring is employed to monitor the time dependent population of the  $^3P_0$  state. The experimental value  $A_{\text{HFI}} = 0.56(3) \text{ s}^{-1}$  is almost 60% larger than theoretically predicted.

DOI: [10.1103/PhysRevLett.98.033001](https://doi.org/10.1103/PhysRevLett.98.033001)

PACS numbers: 32.70.Cs, 31.30.Gs, 34.80.Lx

Atoms and ions in metastable excited states with very small electromagnetic transition rates are promising systems for realizing ultraprecise atomic clocks, for the diagnostic of astrophysical media regarding the competition of radiative and nonradiative processes, for realizing novel types of cold atomic gases, and for probing fundamental correlation effects in the bound states of few-electron systems. In particular, in alkaline-earth-like and, in general, divalent atoms and ions, having a  $(ns)^2^1S_0$  ground state and a valence shell  $n$ , the first excited level above the ground state is the term  $nsnp^3P_0$  (Fig. 1). The absence of a total electronic angular momentum  $J$  for this level makes its single photon decay to the ground state impossible except for the hyperfine induced decay in the case of a nucleus with a spin  $I \neq 0$ . For  $I \neq 0$  the hyperfine interaction mixes states with different  $J$  and the  $nsnp^3P_0$  term acquires a finite but long and strongly isotope-dependent radiative lifetime. These hyperfine-dominated decay rates have been treated theoretically for berylliumlike, magnesiumlike, and zinclike ions [1–4] and for divalent heavier atoms [5,6], where the long and isotope-dependent lifetimes are attractive in view of obtaining ultraprecise optical frequency standards and for cold-atom studies. In low-density astrophysical systems, the fluorescence observed from the hyperfine induced radiative decay of the long-lived  $2s2p^3P_0$  level in the berylliumlike ion  $^{13}\text{C}^{2+}$  can be used to infer the  $^{13}\text{C}:^{12}\text{C}$  abundance ratio, giving insight into stellar nucleosynthesis [7].

Hyperfine-induced (HFI) decay rates in divalent  $nsnp^3P_0$  states were so far determined experimentally only for the atomic-clock transition  $5s5p^3P_0 \rightarrow 5s^2^1S_0$  of  $^{115}\text{In}^+$  in a radio-frequency ion trap [8], with an  $\sim 5\%$  uncertainty, and for the berylliumlike ion  $\text{N}^{3+}$  [9] using observations from a planetary nebula and yielding an uncertainty of 33%. The  $^{115}\text{In}^+$  result is in good agreement with estimates on hyperfine mixing based on experimental spectral parameters of the atom [8], while the  $\text{N}^{3+}$  result, even at its limited precision, allows one to discriminate

between the lifetimes predicted by atomic-structure calculations [1,3] that differ by a factor of almost 4. In view of the large theoretical discrepancies in the atomic-structure based calculations and the scarce experimental data, accurate experimental benchmarks are highly desirable, especially for few-electron systems such as berylliumlike ions with particularly strong correlation effects.

Among the few-electron systems, HFI transitions were also studied for highly charged heliumlike ions [10]. However, in contrast to the present case they represent not only the radiative decay path, but also compete with allowed transitions such as  $1s2p^3P_0 \rightarrow 1s2s^3S_1$ . Moreover, the resulting lifetimes are generally much shorter than in a divalent system with comparable valence shell and nuclear charge; the HFI decay rate variations studied so far for the  $1s2p^3P_0 \rightarrow 1s^2^1S_0$  line are in the range of  $10^7$ – $10^{12} \text{ s}^{-1}$  [11–14].

In the present work we obtain an experimental value for the decay rate of the long-lived  $2s2p^3P_0$  state in  $^{47}\text{Ti}^{18+}$

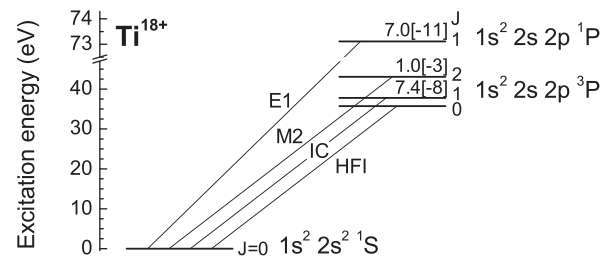


FIG. 1. Simplified level diagram for berylliumlike  $\text{Ti}^{18+}$ . The level energies were taken from the NIST Atomic Spectra Data Base [25], and the lifetimes (in s) labeling the excited levels were calculated from theoretical one-photon transition rates [27] that do not account for hyperfine effects. Numbers in square brackets denote powers of 10. In case of nonzero nuclear spin the hyperfine induced (HFI)  $^3P_0 \rightarrow ^1S_0$  transition rate  $A_{\text{HFI}}$  acquires a finite value. The  $^1P_1 \rightarrow ^1S_0$  electric dipole (E1),  $^3P_2 \rightarrow ^1S_0$  magnetic quadrupole (M2), and  $^3P_1 \rightarrow ^1S_0$  intercombination (IC) transitions are also shown.

( $I = 5/2$ ) through radiative transitions induced by the hyperfine interaction only. This decay limits the lifetime of the  $2s2p^3P_0$  state in  $^{47}\text{Ti}^{18+}$  to  $\sim 1.8$  s. A benchmark HFI decay rate for this highly charged berylliumlike system is obtained with an uncertainty of  $\sim 5\%$  (almost 1 order of magnitude lower than that accomplished previously [9]); the observed decay rate is significantly larger than the only available theoretical prediction [1], which instead would predict a lifetime of  $\sim 2.8$  s. The experiment uses fast, isotopically pure ion beams of  $^{47}\text{Ti}^{18+}$  and  $^{48}\text{Ti}^{18+}$  ( $I = 0$ ) circulating for up to 200 s in the heavy-ion storage-ring TSR of the Max-Planck Institute for Nuclear Physics, Heidelberg, Germany. The new high-resolution electron-ion collision spectrometer [15] at this facility is used to detect a signal proportional to  $\text{Ti}^{18+}$  ions in the metastable  $2s2p^3P_0$  state. For this purpose, the electron-ion collision energy is tuned to a value where dielectronic recombination (DR) occurs only for ions in this excited level, and the rate of recombined  $\text{Ti}^{17+}$  ions produced at this collision energy is recorded as a function of the storage time. This method had been applied previously for measuring the slow radiative decay rates of  $1s2s^3S$  states in the He-like ions ( $\text{B}^{3+}$ ,  $\text{C}^{4+}$ ,  $\text{N}^{5+}$  [16], and  $\text{Li}^+$  [17]).

Mass selected  $^{47,48}\text{Ti}^{18+}$  ion beams (natural abundances 7.2% and 73.7%, respectively) were provided by a tandem accelerator, followed by a radio-frequency linear accelerator, at energies close to 240 MeV, using a fixed magnetic setting for the beam line and the storage ring (magnetic rigidity 0.8533 T m). The residual-gas pressure in the storage ring was  $< 5 \times 10^{-11}$  mbar. In one straight section of the storage ring (circumference  $C = 55.4$  m) the ion beam was continuously phase-space cooled using the velocity-matched electron beam of the TSR electron cooler (electron density  $\sim 5.0 \times 10^7 \text{ cm}^{-3}$ ). In a second straight section, the ion beam was merged with the collinear electron beam of the high-resolution electron target [15], run at variable acceleration voltage in order to set the required collision energy in the comoving reference frame of the ions. At collision energies of 0–2 eV, the electron density in the electron target was  $5.6 \times 10^7 \text{ cm}^{-3}$ .  $\text{Ti}^{17+}$  ions formed by electron-ion recombination in the electron target or by charge transfer in collisions with residual-gas molecules were deflected out of the closed orbit of the circulating  $\text{Ti}^{18+}$  ion beam in the first dipole magnet downstream of the electron target and were directed onto a scintillation detector operated in single-particle counting mode with nearly 100% detection efficiency and negligible dark count rate. The overlap lengths were  $\sim 1.5$  m each in both interaction regions. The cooled ion beam velocities for the two isotopes, as obtained from the space-charge corrected [18] electron acceleration voltage at velocity matching, were  $\beta^{(48)} = 0.1026(1)$  and  $\beta^{(47)} = 0.1047(1)$  (in units of the vacuum speed of light).

Recombination spectra of the  $\text{Ti}^{18+}$  ions as a function of the relative electron-ion energy,  $E_{\text{rel}}$ , were taken by varying

the cathode voltage of the electron target appropriately. The procedure for electron-ion measurements at the TSR storage ring has been described in more detail in, e.g., Ref. [18] (and references therein). For the present spectral measurements, a constant current of cooled, circulating  $\text{Ti}^{18+}$  ions was maintained. Currents of a fraction of a  $\mu\text{A}$  were injected at a rate of  $\sim 1 \text{ s}^{-1}$  in order to obtain stationary stored currents of  $\sim 40 \mu\text{A}$  for  $^{48}\text{Ti}^{18+}$  and  $\sim 6 \mu\text{A}$  for  $^{47}\text{Ti}^{18+}$ , respectively; this largely reflects the difference in the natural isotope abundances. The average storage lifetime in this mode is  $\sim 50$  s.

Figure 2 shows a region of the recombination spectrum where resonances of metastable  $\text{Ti}^{18+}$  ( $2s2p^3P_0$ ) ions occur close to a strong resonance from ground-state  $\text{Ti}^{18+}$  ions. Theoretical calculations using the AUTOSTRUCTURE code [19] were performed to assign the weaker structures to the metastables, which decay by collisional interactions for only the  $^{48}\text{Ti}^{18+}$  beam [Fig. 2(a)]. Using a  $^{47}\text{Ti}^{18+}$  beam [Fig. 2(b)], the resonances assigned to metastable  $\text{Ti}^{18+}$  ( $2s2p^3P_0$ ) ions essentially disappear, as their average population is strongly reduced through the radiative decay (expected life time 2.8 s [1]). The isotope-dependent occurrence of DR resonances was also observed in earlier TSR experiments, using the heavier divalent ion  $\text{Pt}^{48+}$  (Zn-like) [20]. The AUTOSTRUCTURE calculations of the recombination spectrum indicate an average population of  $\sim 5\%$  for the metastable  $\text{Ti}^{18+}$  ( $2s2p^3P_0$ ) ions in the stored  $^{48}\text{Ti}^{18+}$  beam. A similar average population of the  $2s2p^3P_0$  metastable state was found in a recent DR experiment with Be-like  $^{56}\text{Fe}^{22+}$  [21].

For the determination of the time constant associated with the hyperfine quenching the decay of the  $^{47}\text{Ti}^{18+}$  ( $^3P_0$ ) beam component was monitored as a function of storage

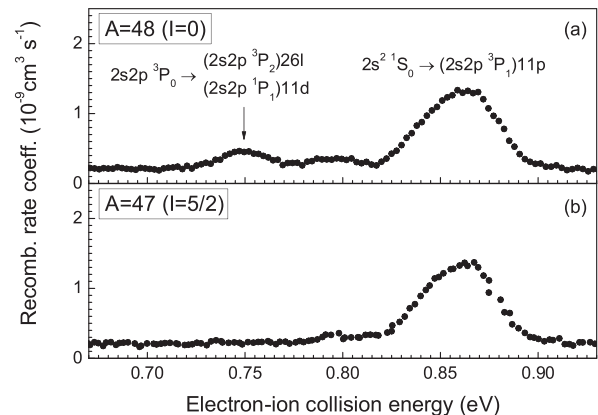


FIG. 2. Measured rate coefficients for the electron-ion recombination of  $^{48}\text{Ti}^{18+}$  (a) and  $^{47}\text{Ti}^{18+}$  (b) in the energy range of interest. The resonances that are formed by resonant dielectronic capture of the initially free electron are assigned to doubly excited  $\text{Ti}^{17+}$  states as indicated with the aid of theoretical calculations using the AUTOSTRUCTURE code [19]. A comprehensive plot of the  $^{48}\text{Ti}^{18+}$  recombination spectrum extending over the entire experimental energy range of 0–80 eV can be found in Ref. [28].

time. To this end the relative electron-ion energy in the electron target was set fixed to 0.75 eV where a DR resonance associated with excitation of the  $^3P_0$  state occurs [vertical arrow in Fig. 2(a)]. After injection of a single  $\text{Ti}^{18+}$  ion pulse into the storage ring, the recombination rate was recorded for up to 200 s. Prior to the injection of the next pulse the remaining ions were kicked out of the ring. This scheme was repeated to reduce statistical uncertainties to a suitable level.

Figure 3 displays the two decay curves that were obtained for the two isotopes with  $A = 48$  and  $A = 47$ . Since the recombination signal was produced by both  $^1S_0$  and  $^3P_0$  ions, the sum of two exponentials, i.e., the function

$$F^{(A)}(t) = c_m^{(A)} e^{-\lambda_m^{(A)} t} + c_g^{(A)} e^{-\lambda_g^{(A)} t}, \quad (1)$$

was fitted to the measured decay curves [16,17]. As discussed in more detail below, the  $^1S_0$  state contributes also at  $E_{\text{rel}} = 0.75$  eV to the measured recombination signal by nonresonant radiative recombination and by electron capture from the residual gas. The fit results are listed in Table I. The one-sigma confidence limits (numbers in parentheses) on the fit parameters  $c_m^{(A)}$ ,  $\lambda_m^{(A)}$ ,  $c_g^{(A)}$ , and  $\lambda_g^{(A)}$  were obtained by Monte Carlo simulations [22] of 100 synthetic data sets for each isotope.

The interpretation of the fitted decay constants in terms of atomic transition rates is straightforward if the rate for collisional excitation of the  $^3P_0$  state during collisions of the  $\text{Ti}^{18+}$  ions with residual-gas particles is negligibly small. Collisional excitation has been investigated in previous experimental measurements of metastable state lifetimes, e.g., with stored  $\text{Xe}^+$  [23],  $\text{C}^{4+}$  [16], and  $\text{Li}^+$  [17] ions. In all these cases collisional processes were found to have a negligibly small influence on the population of the

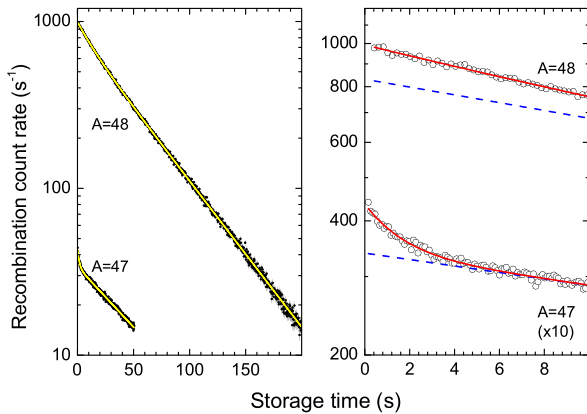


FIG. 3 (color online). Measured  $^{48}\text{Ti}^{17+}$  and  $^{47}\text{Ti}^{17+}$  recombination count rates as a function of storage time. Both panels show the same curves on different time scales. Clearly, the  $A = 47$  curve has a fast decaying component that is absent in the  $A = 48$  curve. The solid lines are the results of the fits of Eq. (1) to the experimental data points (symbols). In the right panel the fitted  $c_g^{(A)} \exp(-\lambda_g^{(A)} t)$  components are shown as dashed lines. The fit results are summarized in Table I.

metastable states under investigation, mainly because of the low residual particle density in the ultrahigh vacuum of the storage ring. Since the residual-gas pressure and the collisional excitation cross sections of the present experiment and of the above mentioned studies are of the same order of magnitude, collisional excitation and deexcitation processes are assumed to be negligible within the experimental uncertainty.

With this assumption the fitted rate constants can be expressed as [16]

$$\lambda_g^{(A)} = A_{gl}^{(A)} \quad \text{and} \quad \lambda_m^{(A)} = A_r^{(A)} + A_{\text{DC}} + A_{ml}^{(A)}, \quad (2)$$

where  $A_r$  is the radiative decay rate of the  $^3P_0$  state and  $A_{\text{DC}}$  is the decay rate of this state due to dielectronic capture (DC) into the  $(2s2p^1P_1)11d$  and  $(2s2p^3P_2)26l$  doubly excited states (Fig. 2). Loss of  $^3P_0$  ions occurs if these states decay either via photon emission (in this case DR has occurred) or via autoionization to the  $2s^2^1S_0$  ground state. Since DC and the subsequent relaxation processes are not significantly influenced by hyperfine effects, the rate  $A_{\text{DC}}$  is the same for both isotopes. The rates  $A_{gl}$  and  $A_{ml}$  describe the loss of the  $^1S_0$  ground state and of  $^3P_0$  metastable ions, respectively, from the storage ring. The most important processes that lead to the loss of ions from the storage ring are collisions with residual-gas particles and electron-ion recombination in the electron cooler.

The loss rate  $A_{gl}$  is different for the two isotopes because the  $^{47}\text{Ti}^{18+}$  and  $^{48}\text{Ti}^{18+}$  ions are stored with different velocities  $v$  and because of the velocity dependence of the relevant cross sections  $\sigma$ . With  $\sigma \propto v^{-x}$  it follows that  $A_{gl} \propto v\sigma \propto v^{1-x}$ . The exponent  $x$  can be determined from  $A_{gl}^{(48)}/A_{gl}^{(47)} = [\beta^{(48)}/\beta^{(47)}]^{1-x}$  yielding  $x = 10(1)$ . This value is consistent with the empirical  $v^{-9.6}$  scaling [24] of the cross section for charge capture during collisions of highly charged ions with neutral residual-gas particles.

The ionization energies of the  $^3S_0$  ground state and the  $^3P_0$  metastable state, 1346 and 1310 eV, respectively [25], differ by less than 3%. Therefore, it can safely be assumed that the loss rates for both states are approximately equal, i.e., that  $A_{ml} = A_{gl}$ . This assumption does not lead to any serious consequences. As will be shown below, the final result for the HFI transition rate changes only insignificantly when, e.g.,  $A_{ml} = 2A_{gl}$  is assumed.

TABLE I. Results (including statistical uncertainties) for the decay constants  $\lambda_{m,g}^{(A)}$  and relative weights  $c_{m,g}^{(A)}$  obtained from the fits of Eq. (1) to the experimental decay curves (Fig. 3).

Isotope	$\lambda_m^{(A)}$ (s <sup>-1</sup> )	$\lambda_g^{(A)}$ (s <sup>-1</sup> )	$c_m^{(A)}$ (s <sup>-1</sup> )	$c_g^{(A)}$ (s <sup>-1</sup> )
$A = 48$	0.070(2)	0.0202(5)	161(35)	831(48)
$A = 47$	0.62(3)	0.016 65(6)	9.8(3)	33.86(6)

With the assumption of  $A_{ml} = A_{gl}$ , Eq. (2) can be solved for  $A_r$  yielding  $A_r^{(A)} = \lambda_m^{(A)} - \lambda_g^{(A)} - A_{DC}$ . Since  $A_r^{(48)} = 0$ , the DC rate is  $A_{DC} = \lambda_m^{(48)} - \lambda_g^{(48)} = 0.050(2) \text{ s}^{-1}$ . Finally, the HFI transition rate of the  $^{47}\text{Ti}^{18+}$  state is calculated as

$$\begin{aligned} A_{\text{HFI}} &= \gamma^{(47)} A_r^{(47)} = \gamma^{(47)} [\lambda_m^{(47)} - \lambda_g^{(47)} - A_{DC}] \\ &= \gamma^{(47)} [\lambda_m^{(47)} - \lambda_g^{(47)} - \lambda_m^{(48)} + \lambda_g^{(48)}], \end{aligned} \quad (3)$$

where the relativistic factor  $\gamma^{(47)} = [1 - (\beta^{(47)})^2]^{-1/2} = 1.00531(1)$  occurs because of the transformation into the ion's frame of reference. With the values for  $\lambda_{m,g}^{(A)}$  from Table I one obtains  $A_{\text{HFI}} = 0.56(3) \text{ s}^{-1}$ . With the assumption of  $A_{ml} = 2A_{gl}$  (see above) the result would change to  $A_{\text{HFI}} = 0.54(3) \text{ s}^{-1}$ . This change is within the experimental uncertainty which is mainly determined by the statistical uncertainty of  $\lambda_m^{(47)}$  (Table I). It shows the relatively low sensitivity of the experimental radiative rate on the difference between  $A_{ml}$  and  $A_{gl}$ .

The remaining issue to be discussed is the possible quenching of the  $^3P_0$  state in the magnetic fields of the storage-ring magnets [26] via the  $B$ -field induced mixing of the  $^3P_0$  state with the  $^3P_1$  state. The magnitude of the mixing coefficient is of the order of  $\mu_B B / \Delta E$ , where  $\mu_B$  is the Bohr magneton and  $\Delta E$  is the  $^3P_0 - ^3P_1$  energy splitting. For the present experiment it is estimated that the  $^3P_0 \rightarrow ^1S_0$  transition rate by  $B$ -field induced mixing is more than 2 orders of magnitude smaller than  $A_{\text{HFI}}$ . Therefore, it can safely be neglected.

The present experimental value  $A_{\text{HFI}} = 0.56(3) \text{ s}^{-1}$  for the hyperfine induced  $^3P_0 \rightarrow ^1S_0$  transition rate in Be-like  $^{47}\text{Ti}^{18+}$  with  $I = 5/2$  is 57% larger than the theoretical value of  $0.3556 \text{ s}^{-1}$  [1]. It has been shown that calculated values of  $A_{\text{HFI}}$  are very sensitive to electron-electron correlation [3]. If correlation is treated more thoroughly, HFI transition rates larger by factors of up to 4 [3] (see above) are obtained as compared with a less extensive treatment [1]. Therefore, the present discrepancy between experiment and theory is ascribed to a partial neglect of important correlation effects in the theoretical calculation.

In summary, in this work an experimental value from a laboratory measurement is presented for the very low hyperfine induced  $^3P_0 \rightarrow ^1S_0$  transition rate in Be-like  $\text{Ti}^{18+}$ . It is almost 1 order of magnitude more precise than the only previous experimental value for isoelectronic  $\text{N}^{3+}$  [9] that was obtained from astrophysical observations and modeling. The present value for the HFI transition rate exceeds the only presently available theoretical result [1] by 57%. This difference is attributed to electron correlation effects that were included only approximately in the theoretical calculation. An essential feature of the present experimental method is the comparison of measured re-

sults from different isotopes with zero and nonzero nuclear spin. The method is readily applicable to a wide range of ions and has the potential for yielding even more accurate results.

The authors thank M. Schnell for a helpful discussion and gratefully acknowledge the excellent support by the MPI-K accelerator and TSR crews. This work was supported in part by the German federal research-funding agency DFG under Contract No. Schi 378/5.

---

\*Permanent address: Institute of Modern Physics, Chinese Academy of Sciences, Lanzhou 730000, People's Republic of China.

- [1] J. P. Marques, F. Parente, and P. Indelicato, *Phys. Rev. A* **47**, 929 (1993).
- [2] J. P. Marques, F. Parente, and P. Indelicato, *At. Data Nucl. Data Tables* **55**, 157 (1993).
- [3] T. Brage *et al.*, *Astrophys. J.* **500**, 507 (1998).
- [4] Y. Liu *et al.*, *J. Phys. B* **39**, 3147 (2006).
- [5] S. G. Porsev and A. Derevianko, *Phys. Rev. A* **69**, 042506 (2004).
- [6] R. Santra, K. V. Christ, and C. H. Greene, *Phys. Rev. A* **69**, 042510 (2004).
- [7] R. H. Rubin, G. J. Ferland, E. E. Cholle, and R. Horstmeier, *Astrophys. J.* **605**, 784 (2004).
- [8] T. Becker *et al.*, *Phys. Rev. A* **63**, 051802(R) (2001).
- [9] T. Brage, P. G. Judge, and C. R. Proffitt, *Phys. Rev. Lett.* **89**, 281101 (2002).
- [10] H. Gould, R. Marrus, and P. J. Mohr, *Phys. Rev. Lett.* **33**, 676 (1974).
- [11] L. Engström *et al.*, *Phys. Scr.* **22**, 570 (1980).
- [12] R. W. Dunford *et al.*, *Phys. Rev. A* **44**, 764 (1991).
- [13] P. Indelicato *et al.*, *Phys. Rev. Lett.* **68**, 1307 (1992).
- [14] B. B. Birkett *et al.*, *Phys. Rev. A* **47**, R2454 (1993).
- [15] F. Sprenger *et al.*, *Nucl. Instrum. Methods Phys. Res., Sect. A* **532**, 298 (2004).
- [16] H. T. Schmidt *et al.*, *Phys. Rev. Lett.* **72**, 1616 (1994); H. T. Schmidt, Ph.D. thesis, University of Aarhus, 1994.
- [17] A. A. Saghiri *et al.*, *Phys. Rev. A* **60**, R3350 (1999).
- [18] S. Kieslich *et al.*, *Phys. Rev. A* **70**, 042714 (2004).
- [19] N. R. Badnell, *J. Phys. B* **19**, 3827 (1986).
- [20] S. Schippers *et al.*, *Nucl. Instrum. Methods Phys. Res., Sect. B* **235**, 265 (2005).
- [21] D. W. Savin *et al.*, *Astrophys. J.* **642**, 1275 (2006).
- [22] W. H. Press *et al.*, *Numerical Recipes in C++* (Cambridge University Press, New York, USA, 2002), Chap. 15.6.
- [23] S. Mannervik *et al.*, *Phys. Rev. A* **56**, R1075 (1997).
- [24] A. S. Schlachter *et al.*, *Phys. Rev. A* **27**, 3372 (1983).
- [25] Y. Ralchenko *et al.*, NIST Atomic Spectra Database, version 3.0.2, available at <http://physics.nist.gov/asd3>.
- [26] S. Mannervik *et al.*, *Phys. Rev. Lett.* **76**, 3675 (1996).
- [27] A. K. Bhatia, U. Feldman, and G. A. Doschek, *J. Appl. Phys.* **51**, 1464 (1980).
- [28] S. Schippers *et al.*, physics/0609072.